a single wavelength regime (for example, the UV). In this arrangement, the viewing angle is determined by the emission of the polarized PL layer, which is less angle-dependent than are LC effects. Switching of this device changed the brightness from 8 to 4 cd m^{-2}. The limited contrast and absolute brightness of the "on" and "off" states relative to those of devices A and B are attributable to the limited transparency of the commercial UV sheet polarizer that was used (about 22% at 365 nm) and, of course, the slightly lower dichroic ratio (*15*) of the polarized PL layer in absorption relative to emission (*22*). A clearly improved viewing angle was observed when comparing device C (>170°) with devices A and B (<130°).

Many other device configurations based on polarized PL layers can be envisioned, such as reflective-mode direct-view displays in which ambient light functions as the light source, pixilated multicolor structures, or stacks of multiple EO light valves and polarized PL layers (*15*). Although TN LC cells were used for all devices described above, the present concepts equally apply to displays based on alternative systems, such as electrically controlled birefringence or supertwisted nematic effect LC cells. Although green light– and orange-red light–emitting PL display devices have been demonstrated in this work, other colors (such as blue) can also be readily produced, because suitable conjugated polymers covering the full visible range are available (*2*). The technology of devices of this type, in which light emitted from the PL layer is switched, is widely compatible with commercially used backlit displays and might readily be adapted. In contrast, polarizers and LC cells of improved stability and transparency are required for the technological use of devices in which excitation light is switched.

REFERENCES AND NOTES

1. For a recent review, see H. Kobayashi, *Proc. SPIE* **1910**, 15 (1993).
2. For a recent review, see D. Bradley, *Curr. Opin. Solid State Mater. Sci.* **1**, 789 (1996).
3. L. K. M. Chan, in *The Encyclopedia of Advanced Materials*, D. Bloor, R. J. Brook, M. C. Flemings, S. Mahajan, Eds. (Elsevier Science, Oxford, 1994), vol. 2, pp. 1294–1304.
4. F. Funada, M. Matsuura, T. Wada, U.S. Patent 4 336 980 (1982); H. J. Coles, *Liq. Cryst.* **14**, 1039 (1993).
5. G. Baur and W. Greubel, *Appl. Phys. Lett.* **31**, 4 (1977); M. Bechtler and H. Krüger, *Electronics* **50**, (25), 113 (1977).
6. W. A. Crossland, I. D. Springle, A. B. Davey, *Proc. SID Symp. Digest of Technical Papers* (Society for Information Display, Santa Ana, CA, 1997), vol. 27, pp. 837–840.
7. E. Lommel, *Ann. Phys. Chem.* **8**, 634 (1879).
8. T. W. Hagler *et al.*, *Polymer Comm.* **32**, 339 (1991); T. W. Hagler, K. Pakbaz, A. J. Heeger, *Phys. Rev. B* **44**, 8652 (1991).
9. P. Dyreklev *et al.*, *Adv. Mater.* **7**, 43 (1995); G. Lüssem *et al.*, *Liq. Cryst.* **21**, 903 (1996); V. Cimrova, M. Remmers, D. Neher, G. Wegner, *Adv. Mater.* **8**, 146 (1996).
10. D. Steiger, P. Smith, Ch. Weder, *Makromol. Chem. Rapid Commun.* **18**, 643 (1997).
11. Ch. Weder and M. S. Wrighton, *Macromolecules* **29**, 5157 (1996); A. Montali, Ch. Weder, P. Smith, *Proc. SPIE*, **3148**, 298 (1997). For a recent review on PPEs, see also R. Giesa, *J. Macromol. Sci. Rev. Macromol. Chem. Phys.* **C36**, 631 (1996).
12. Ch. Weder, C. Sarwa, C. Bastiaansen, P. Smith, *Polym. Prepr. Am. Chem. Soc. Div. Polym. Chem.* **38**, 404 (1997); *Adv. Mater.* **9**, 1035 (1997).
13. Blend films were prepared by casting a solution of the PPE (10 mg) and UHMW-PE (Hostalen Gur 412, Hoechst, 0.5 g) in xylene (50 ml) (dissolution at 130°C, after degassing the mixture in vacuum at 25°C for 15 min) into a petri dish 11 cm in diameter. The resulting gels were dried under ambient conditions for 24 hours to yield films of a homogeneous thickness of about 70 μm. These blend films were drawn at temperatures of 90° to 120°C to a draw ratio λ (final length/initial length) of about 80, to produce oriented PL layers of a thickness of about 2 μm. The PL layers were sandwiched between two glass or quartz slides; a thin layer of silicon oil fluid was applied to minimize light scattering at the film surfaces. Further details on the preparation of polarized PL layers are given in (*12*).
14. F. Wudl and G. Srdanov, U.S. Patent 5 189 136 (1993).
15. Ch. Weder, C. Bastiaansen, C. Sarwa, P. Smith, European Patent Application No. 97111229.7.
16. We thank D. J. Broer for stimulating discussions and for providing LC cells.

16 September 1997; accepted 23 December 1997

A Rare-Earth Phosphor Containing One-Dimensional Chains Identified Through Combinatorial Methods

Earl Danielson, Martin Devenney, Daniel M. Giaquinta,
Josh H. Golden,* Robert C. Haushalter, Eric W. McFarland,
Damodara M. Poojary, Casper M. Reaves, W. Henry Weinberg,†
Xin Di Wu

An unusual luminescent inorganic oxide, Sr_2CeO_4, was identified by parallel screening techniques from within a combinatorial library of more than 25,000 members prepared by automated thin-film synthesis. A bulk sample of single-phase Sr_2CeO_4 was prepared, and its structure, determined from powder x-ray diffraction data, reveals one-dimensional chains of edge-sharing CeO_6 octahedra, with two terminal oxygen atoms per cerium center, that are isolated from one another by Sr^{2+} cations. The emission maximum at 485 nanometers appears blue-white and has a quantum yield of 0.48 ± 0.02. The excited-state lifetime, electron spin resonance, magnetic susceptibility, and structural data all suggest that luminescence originates from a ligand-to-metal Ce^{4+} charge transfer.

Combinatorial material synthesis allows large libraries to be prepared for systematic study and identification of promising lead materials. Initial studies of inorganic materials already suggest that for superconducting (*1*), magnetoresistive (*2*), and photoluminescent (*3*) solids combinatorial techniques can identify materials with superior properties among numerous similar congeners. To date, however, these studies have focused primarily on the synthesis of compositional variants, often with relatively shallow variable gradations, to optimize known properties within classes of materials with previously known structure types. We have prepared and characterized a fundamentally new type of luminescent material, Sr_2CeO_4, in which only combinatorial techniques were used to determine the elemental composition. Subsequent studies, after preparation of bulk samples of this lead composition, showed it to possess an unusual one-dimensional chain structure type, not previously seen for a luminescent rare-earth–based oxide, that is intimately related to the charge transfer mechanism by which Sr_2CeO_4 luminesces.

The luminescent phase Sr_2CeO_4 was identified by automated high-throughput screening techniques from within a discovery library of over 25,000 compositionally independent elements that was prepared by electron beam evaporation with multiple targets and moving masks (*3*). Screening for candidate materials was performed using a charge-coupled device (CCD) camera, as previously described (*3*). Comparison of the visible emission of a subsection of the library under 254-nm excitation (Fig. 1) with that of known luminescent materials identified the blue-white emission from the Sr-, Sn-, and Ce-containing region (upper right corner) as a potentially new phosphor material. A subsequent ternary focus library containing combinations of these three elements revealed that Sn was not needed for

---

Symyx Technologies, 3100 Central Expressway, Santa Clara, CA 95051, USA.
The authors all contributed equally to this work.

*Present address: Semiconductor Equipment Group, Watkins-Johnson, 440 Kings Village Road, Scotts Valley, CA 95066–4081, USA.
†To whom correspondence should be addressed. E-mail: hweinberg@symyx.com

the observed emissive properties, and that maximum luminosity was observed at Sr:Ce ratios greater than unity.

As suggested by the focus library, and assuming Ce to be in the 4+ oxidation state under these synthetic conditions, a bulk sample with a 2:1 ratio of Sr:Ce was prepared from the reaction of CeO_2 with $SrCO_3$ for 48 hours at 1000°C in air, with four intermediate regrindings, in order to study the optical and other physical properties. The excitation and emission spectra of Sr_2CeO_4 displayed broad maxima at 310 and 485 nm, respectively, with the emission appearing blue-white to the eye (CIE 1931 chromaticity coordinates $x = 0.198$, $y = 0.292$). This phosphor is effectively excited by x-rays and exhibits efficient cathodoluminescence (5.1 lm/W at 20 kV and 1 $\mu A/cm^2$). Unlike most other rare earth–based oxide phosphors, the emission from Sr_2CeO_4 is quite broad and has an uncharacteristically long excited-state lifetime (51.3 ± 2.4 μs) compared with *d-f* transitions within the Ce^{3+} excited states. Because the Ce atom would be expected to be in the 4+ oxidation state under the given synthetic conditions, and because all known Ce-based phosphors emit from localized Ce^{3+} states, a structural study of Sr_2CeO_4 was undertaken to clarify further the relations of the optical properties to the structure.

The composition Sr_2CeO_4 (required from the 2:1 Sr:Ce ratio and the presumption of Ce^{4+}) has been reported (*4*) to be in the triclinic crystal system in space group $P\bar{1}$ with cell parameters $a = 6.070$ Å, $b = 8.976$ Å, $c = 10.598$ Å, $\alpha = 94.7°$, $\beta = 90.4°$, and $\gamma = 95.8°$. We have indexed our Sr_2CeO_4 samples to an orthorhombic cell with $a = 6.11897(9)$ Å, $b = 10.3495(2)$ Å, and $c = 3.5970(1)$ Å (numbers in parentheses are the errors in the last digits) and believe that the previously described material (*4*) was in fact the same as ours but that the unit cell was incorrectly indexed because certain key weak reflections were omitted. The correctness of our orthorhombic cell is confirmed by the structure solution obtained from powder x-ray diffraction data in space group *Pbam* and the high quality of the Rietveld refinement of the structure (*5*). The structure of Sr_2CeO_4 is highly anisotropic and is an unusual phosphor in that it contains one-dimensional chains. The structure (Fig. 2) consists of linear chains of edge-sharing CeO_6 octahedra that run parallel to the [001] crystallographic direction with a repeat distance of 3.597 Å. The most notable feature of the linear chain of octahedra is the presence of two trans terminal Ce-O groups perpendicular to the plane defined by the four equatorial μ^2-O atoms. As expected, the terminal Ce-O bonds are slightly shorter than the equatorial bonds by ~0.1 Å.

We believe that this low-dimensional structure, with its terminal Ce-O bonds, is critical to the observation of luminescence in Sr_2CeO_4 and that the mechanism of luminescence is based on ligand-to-metal charge transfer, from O^{2-} to Ce^{4+}, and not transitions arising from isolated valence transitions from Ce^{3+} defect centers. The chemical formula of Sr_2CeO_4 suggests that all Ce atoms should be present as Ce^{4+}. Magnetic susceptibility measurements indicate that single-phase samples of Sr_2CeO_4 are essentially diamagnetic between 4 and 300 K (paramagnetic impurities corresponding to only $\sim 10^{-3}$ μ_B mol^{-1} per Ce atom, where μ_B is the Bohr magneton), and electron spin resonance (ESR) measurements also confirm that no significant amount of Ce^{3+} is present. This concentration of Ce^{3+} is far too low to account for the luminosity observed from Sr_2CeO_4. Thermogravimetric experiments in air show little loss up to 1000°C, indicating that there is no easily removable lattice oxygen under these conditions and suggesting little tendency toward a highly defected oxide lattice. These results, combined with the anomalous (for Ce^{3+}) lifetime, strongly suggest that the mechanism of emission in Sr_2CeO_4 is not based on Ce^{3+}.

A possible emissive pathway is suggested by comparison of the crystal structure of Sr_2CeO_4 with that of the perovskite structure of $SrCeO_3$, which does not luminesce. In the former linear chain compound, four of the six O atoms of the octahedrally coordinated Ce are coordinated in a μ^2 fashion to two adjacent Ce centers (Ce^{4+}-O-Ce^{4+}), with the remaining two terminal O atoms bonded to only one Ce^{4+}. In $SrCeO_3$, which has a three-dimensional $CeO_{6/2}$ oxide framework with each Ce^{4+} sharing all corners with six neighboring octahedra, as in the ReO_3 structure type, every O atom is coordinated to two Ce^{4+}centers in a Ce^{4+}-O-Ce^{4+} fashion. An excited state based on O^{2-} to Ce^{4+} ligand-to-metal charge transfer (that is, one with "Ce^{3+}-O^{1-}" character) may be possible when a relatively electron-rich terminal O atom is bound to a single oxidizing Ce^{4+} center, as in Sr_2CeO_4, but not when all O atoms are bound to two Ce^{4+}, as in $SrCeO_3$. Thus, the charge transfer results from the lower coordination number terminal O atoms associated with the low-dimensional structure, in combination with an adjacent Ce^{4+} center, and suggests that luminescence might also be found among other rare earth–based materials with similar structural features. Charge transfer of this type has been noted previously in rare earth compounds (*6*),

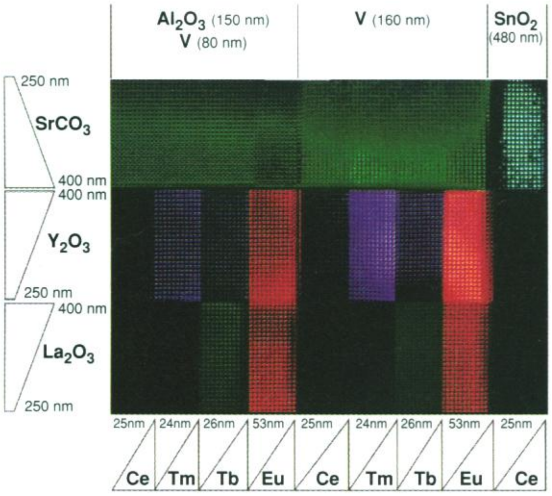

Fig. 1. Image of the ultraviolet-excited (254 nm) photoluminescence from a section of a diverse discovery library containing ~25,000 different compositions. In the complete library, four columns were deposited first with constant thicknesses of SnO_2, V, Al_2O_3:V (15:8 molar ratio), and Al_2O_3. Four rows with linearly varying thicknesses of La_2O_3, Y_2O_3, MgO, and $SrCO_3$ were then layered on the columns to divide the substrate into 16 host lattice subregions. Finally, within each subregion, columns of rare earth oxides Eu_2O_3, Tb_4O_7, Tm_2O_3, and CeO_2 were deposited with linearly varying thicknesses. The thicknesses of the different library hosts and dopants varied across the regions, as indicated. A primary mask used during deposition separated the library into 230-μm-square elements spaced 420 μm apart. The blue-white emission in the upper right corner emanates from Sr_2CeO_4.

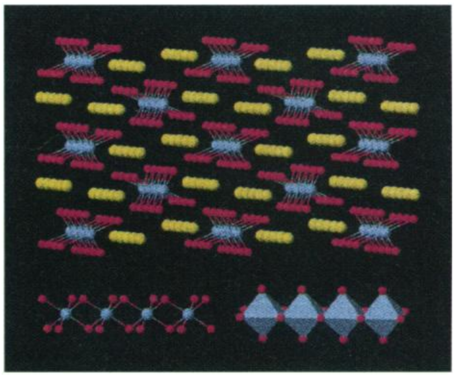

Fig. 2. The structure of Sr_2CeO_4 (viewed down [001]) consists of linear chains of trans edge-sharing CeO_6 octahedra, with four equatorial μ^2-O atoms and two terminal Ce-O bonds per octahedron, surrounded by interchain Sr^{2+} cations. The O atoms are red; Ce, light blue; and Sr, yellow.

mainly Ce-, Pr-, and Tb-based materials, in which 4+ and 3+ oxidation states are accessible. Although no visible luminescence was observed in any of these materials, none of them allowed the M^{4+} cation to exist in a coordination environment where terminal M-O bonds exist. Scheelite as well as other minerals and synthetic materials containing high–oxidation state metal ions also luminesce by charge-transfer type mechanisms (*7*).

To ascertain if there were other luminescent phases within the M_2CeO_4 (M = Ba, Ca, and Mg) phase space, a triangular library was prepared with the M_2CeO_4 compositions at each corner. This library was prepared by robotically dispensed sol-gel precursors and followed by heating to 900°C. Under 254-nm excitation (Fig. 3), the Sr-containing region has the brightest emission, and there is no appreciable luminosity from the Ba and Mg regions. Once the stable sol-gel precursors were synthesized, deposition of the library took ~15 to 20 min. Powder x-ray diffraction of the individual elements confirmed that no additional phases isotypic to Sr_2CeO_4 exist on this library.

Although combinatorial methods might initially appear to be limited to substitutional variants of existing materials, this work shows that unexpected structures can be identified. After isolation, structural and spectroscopic studies showed that Sr_2CeO_4 possesses a phosphor structure type that emits light not by the usual mechanism originating from within the electronic states of a paramagnetic rare-earth site, but rather from a charge-transfer mechanism. The identification of a material displaying a property (luminescence) that arises through an unusual mechanism illustrates the possibilities that the combinatorial approach can open in materials science.

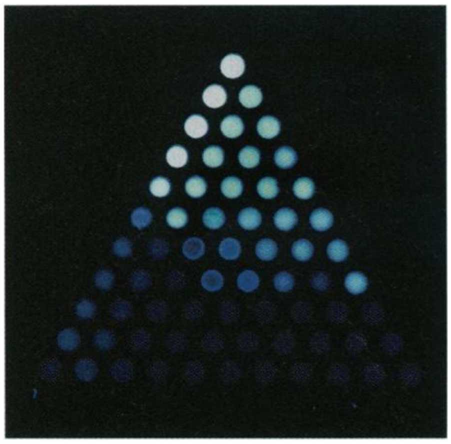

Fig. 3. Photograph of a ternary M_2CeO_4 (M = Ca, Sr, and Ba) library under 254-nm excitation. The Ce concentration in each element is constant, and the M gradient decreases linearly from the corner of the pure M_2CeO_4 composition in a direction along the bisector of the opposite edge. Element map: Sr, top; Ba, lower left; and Ca, lower right.

REFERENCES AND NOTES

1. X.-D. Xiang *et al.*, *Science* **268**, 1738 (1995).
2. G. Briceño, H. Chang, X. Sun, P. G. Schultz, X.-D. Xiang, *ibid.* **270**, 273 (1995).
3. E. Danielson *et al.*, *Nature* **389**, 944 (1997).
4. M. D. Mastromonaco, I. Barbariol, A. Cocco, *Ann. Chim.* (*Rome*) **59**, 465 (1969).
5. Step-scanned x-ray powder diffraction data for the sample were collected with the use of a 9-kW rotating anode generator equipped with a copper target and graphite monochromator. Data were collected in the 2θ range from 15° to 110° with a step size of 0.01° and a count time of 6 s per step. The powder pattern was indexed by standard methods. Space group *Pbam*, a = 6.11897(9) Å, b = 10.3495(2) Å, and c = 3.5970(1) Å. The intensities were extracted using the program EXTRA [A. Altomore *et al.*, *J. Appl. Crystallogr.* **28**, 842, (1995)], and the structure was solved ab initio using SIRPOW [A. Altomore *et al.*, *Acta Crystallogr. A* **47**, 744 (1991)]. Full-pattern Rietveld refinement was carried out using the program GSAS. Final refinement converged with R_{wp} = 0.081, R_p = 0.059, and R_F = 0.026 for 172 independent observations.
6. H. E. Hoeffdraad, *J. Inorg. Nucl. Chem.* **37**, 1917 (1975).
7. G. Blasse and B. C. Grabmaier, *Luminescent Materials* (Springer-Verlag, Berlin, 1994); J. L. Ouweltjes, "Luminescence and Phosphors," *Modern Materials* **5**, 161 (1965).

8. This work would not have been possible without technical assistance from G. Wallace-Freedman, Y. Wang, and J. Wu. The authors also acknowledge helpful advice from J. McCusker and S. Jacobsen. We are grateful for the ESR measurements performed by B. Warren (Sandia National Laboratory). The experimental details for the preparation and processing of the focus and discovery libraries as well as the crystallographic data are available as supplementary material at www.sciencemag.org/feature/data/975265.shl

29 September 1997; accepted 23 December 1997

Frictional Melting During the Rupture of the 1994 Bolivian Earthquake

Hiroo Kanamori, Don L. Anderson, Thomas H. Heaton

The source parameters of the 1994 Bolivian earthquake (magnitude M_w = 8.3) suggest that the maximum seismic efficiency η was 0.036 and the minimum frictional stress was 550 bars. Thus, the source process was dissipative, which is consistent with the observed slow rupture speed, only 20% of the local *S*-wave velocity. The amount of nonradiated energy produced during the Bolivian rupture was comparable to, or larger than, the thermal energy of the 1980 Mount St. Helens eruption and was sufficient to have melted a layer as thick as 31 centimeters. Once rupture was initiated, melting could occur, which reduces friction and promotes fault slip.

The possibility of frictional melting during faulting has been suggested by several investigators (*1–4*). McKenzie and Brune (*2*) quantitatively investigated this problem as a one-dimensional heat conduction problem. They assumed that the fault surface is simultaneously heated during slippage (that is, infinite rupture speed) over a finite time. The temperature was determined mainly by generation of heat (the integrated product of slip and frictional stress) and diffusion of heat (controlled by duration of the heating event and thermal diffusivity). The duration of heating was determined by the driving stress on the fault. If the driving stress was lower, the heating process was slower, allowing heat to diffuse over a larger distance away from the fault; this case results in less temperature rise. They concluded that if the frictional and driving stresses are of the order of 1 kbar, melting could occur for fault slips as small as 1 mm. Richards (*4*) solved elastodynamic equations for a propagating elliptical crack and estimated the frictional heating rate behind a rupture front. He showed that if the driving stress is 100 bars and the fault particle velocity is 10 cm/s at the time of rupture nucleation, a temperature rise of about 1000°C can occur within a few seconds at a point halfway between the rupture front and the point of nucleation. These studies indicate that frictional melting can occur if the stresses involved in faulting are sufficiently high. Despite these studies, frictional melting is not generally regarded as an important process during earthquake faulting because of uncertainties in the stress levels—especially the magnitude of frictional stresses—associated with earthquakes and uncertainties in the detailed fault-zone structures. Sibson (*3*) noted that production of pseudotachylyte (glassy material presumably formed by frictional melting) should take place during faulting, but very few faults contain pseudo-tachylytes.

The 9 June 1994 M_w = 8.3 Bolivian event (13.86°S, 67.54°W; depth = 637 km) was a large deep-focus earthquake (source parameters shown in Table 1). Although the results obtained by different studies vary in detail, the values of most source parameters

---

Seismological Laboratory, California Institute of Technology, Pasadena, CA 91125, USA.